

Hybrid Magnetoacoustic Method for Breast Tumor Detection: An In-vivo and In-vitro Modelling and Analysis.

MAHEZA IRNA MOHAMAD SALIM, MOHAMMAD AZIZI TUMIRAN, SITI NOORMIZA
MAKHTAR, BUSTANUR ROSIDI, ISMAIL ARIFFIN, ABD HAMID AHMAD, EKO
SUPRIYANTO

Universiti Teknologi Malaysia,
Faculty of Biomedical and Health Science Engineering
Department of Clinical Engineering and Sciences,
81310 Johor Bahru, Johor,
MALAYSIA

maheza@utm.my, iziza_366@yahoo.com, bustanur@fke.utm.my, ismail@fke.utm.my,
abhamid@fke.utm.my, eko@utm.my
<http://www.biomedical.utm.my>

Abstract: A new breast cancer detection method that is based on tissue bioelectric and acoustic characteristics has been developed by using a hybrid magnetoacoustics method. This method manipulates the interaction between acoustic and magnetic energy upon moving ions inside the breast tissue. Analytical in-vivo and in-vitro modelling and analysis on the system performance have been done on normal and pathological mice breast tissue models. Analysis result shows that, hybrid magnetoacoustic method is capable to give unique characteristics between normal and pathological mice breast tissue models especially in in-vitro application. However, additional parameter such as analysis of current distribution in tissue should be taken into account for in-vivo application due to the redundancy of the existing result.

Key-words: magnetic field, acoustic wave, breast tissue, normal and pathological.

1. Introduction

The emergence of magnetoacoustic method, a combination between acoustic and magnetic energy has been explored since 2 decades ago for impedance mapping of tissue [1-8]. Basically, magnetoacoustic method manipulates the interaction that rises when acoustic and magnetic energy acting simultaneously on random ionic particles inside a tissue. Biological tissue is a conductive element due to the presence of random charges that is mainly contributed by intra and extracellular diffusion that supports cell metabolism [1-5]. Propagation of ultrasound wave will cause charges inside the breast tissue to move at high velocity due to the back and forth motion of the wave [25-27]. Moving charges in the present of magnetic field will experience Lorentz Force that separate the positive and negative charges, producing an externally detectable

voltage that can be collected using a couple of skin electrode [1-3].

This interaction has been manipulated to map conductivity data of biological tissue especially in impedance imaging. However, previous researches [1-8] apply magnetoacoustic method for conductivity mapping purposes only. The ultrasound wave that is used to stimulate ionic particle motion is not taken into account though its output delivers valuable information with regards to tissue mechanical properties [9]. Table 1 below summarizes previous research reports that combines ultrasound and magnetic energy.

In ultrasound imaging, detection of malignant and benign breast nodules are often complicates by their mechanical characteristic similarities. Benign and malignant nodules have very small differences in tissue density [10]. Hence

additional information such as tissue conductivity will be very helpful for tissue characterization.

Table 1: Summary of previous research reports that combines ultrasound and magnetic field for impedance mapping of tissue.

| Ref | System | Internal Bioelectric generation method | Output signal |
|-----|---------------------------------------|---|------------------|
| 1-3 | Hall Effect Imaging | Static Magnetic Field + Ultrasound | Voltage |
| 5 | Magneto-Acousto Electrical Tomography | Static Magnetic Field + Focused Ultrasound | Voltage /current |
| 4 | US-Magnetic field | Static Magnetic Field + Ultrasound | Current |
| 7-8 | MATMI | Static magnetic Field + Variable magnetic Field | Ultrasound |

In this study, a hybrid magnetoacoustic method that combines magnetic and acoustic energy has been developed. This system is not only collecting the magnetoacoustic voltage that rises from the acoustic and magnetic energy interaction for conductivity evaluation, it also captured back the ultrasound echo that is initially used to induce charge motion inside the breast tissue for acoustic properties evaluation. This paper describes the in-vivo and in-vitro quantitative analysis through a one dimensional modelling for normal and pathological breast tissue evaluation.

1.1 Theory

Consider a one dimensional example of an ion inside a breast tissue having charge q . An ultrasound transducer delivers a longitudinal ultrasound wave in the x direction perpendicular to magnetic field \mathbf{B}_0 which is in the y direction. The longitudinal particle motion of the ultrasound wave at position x and time t will cause the ion

to oscillate back and forth in the tissue with velocity $\mathbf{v}(x,t)$. In the presence of the constant magnetic field \mathbf{B}_0 , the ion is subjected to Lorentz Force of [1-3]:

$$\mathbf{F} = q\mathbf{v}(x,t) \times \mathbf{B}_0 \quad (1)$$

This force is equivalent to an electric field of:

$\mathbf{E}_0 = \mathbf{v}(x,t) \times \mathbf{B}_0$ (2) That establishes a current density of:

$$\mathbf{J}_0 = \sigma \mathbf{v}(x,t) \times \mathbf{B}_0 \quad (3)$$

Total current is derived by integrating (3) over the transducer beam width W and the ultrasound path [1-3]:

$$I(t) = W \mathbf{B}_0 \int_{\text{soundpath}} \sigma(x) \mathbf{v}(x,t) dx \quad (4)$$

Hence, the resulting voltage collected by the system circuitry with impedance R is [1-3]:

$$V(t) = \alpha R_c W \mathbf{B}_0 \int_{\text{soundpath}} \sigma(x) \mathbf{v}(x,t) dx \quad (5)$$

From the equation, it is known that the amplitude of magnetoacoustic voltage is proportional to the tissue conductivity since another parameter such as \mathbf{v} , \mathbf{B}_0 , α , R and W is controlled by the system. In the present study, the value of R is 600Ω for Ag/AgCl electrodes and α is set to 100% representing an ideal detection circuit.

Using the equation of wave motion, the resulting voltage in (5) can also be expressed in terms of ultrasound pressure and spatial gradient of tissue conductivity and density as [1-3]:

$$V(t) = \alpha W \mathbf{B}_0 \int_{\text{soundpath}} \left[\int p(x,t) \delta\tau \frac{\partial}{\partial x} \left[\frac{\sigma(x)}{\rho(x)} \right] dx \right] \quad (6)$$

Since the resulting voltage is proportional to the tissue conductivity, this information is very valuable to be used in breast tumor characterization since in general; pathological tissue will have higher conductivity compared to normal tissue due to an increased rate of metabolism.

Besides the magnetoacoustic voltage that rises from the acoustic and magnetic energy interaction, the transmitted ultrasound wave packet in the x direction that is initially used to induce ionic particle motion will further propagates inside the breast tissue. The ultrasound

propagation in one dimensional is governed by the wave equation:

$$\frac{\partial^2 \phi}{\partial x^2} - \frac{1}{c_l^2} \frac{\partial^2 \phi}{\partial t^2}$$

In which c_l is the longitudinal speed of sound in breast tissues and ϕ is the velocity potential. As the ultrasound propagates further, part of the wave will be reflected back when it hits tissue boundary and another part will be further transmitted and attenuated inside the tissue. The echoes captured back from the system carry information on wave attenuation and time of flight that is valuable for breast tumor acoustic characterization.

2 Methodology

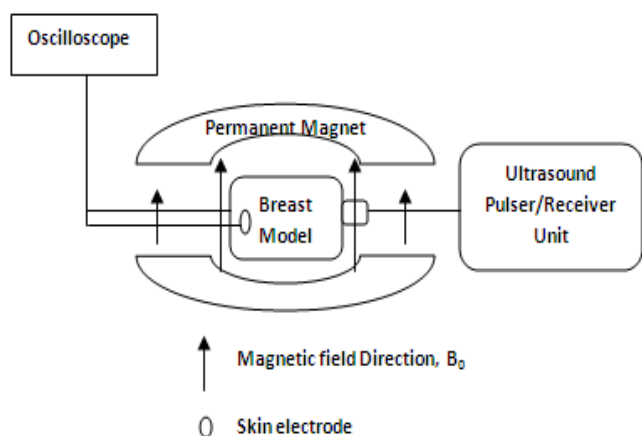


Fig. 1: Calculation set up of Hybrid Magnetoacoustic method.

Figure 1 above shows the calculation set up of the developed system. This system consists of a set of permanent magnet, ultrasound pulser and receiver unit as well as an oscilloscope to collect the voltage data. In this study, a complete mathematical analysis has been done to test the efficiency of the hybrid system in differentiating normal and pathological mice breast tissue models both, in-vitro and in-vivo. Normal and pathological mice breast models having breast carcinoma and benign fibrosis were evaluated in terms of its acoustic and electric characteristics.

2.1 Magnetic Field.

Static magnetic field having intensity of 0.1T is used in the calculation. The magnitude is assumed to be homogenous throughout the breast tissue model. The magnetic field direction is set in positive y direction, perpendicular to the ultrasound wave.

2.2 Ultrasound System

The ultrasound system delivers 10 MHz frequency pulses with amplitude of 200V and repetition frequency of 5000Hz via a PVDF transducer. Since the measured impedance of the PVDF transducer is 1.39e6 Ω , total electrical power delivered by the system is 7.19e-9W. However, total acoustic power received by the tissue is only 1nW due to the low electroacoustic coupling factor of the PVDF. Total acoustic intensity delivered by the system is 3.965e-8 W/cm² with 0.0254cm² beamwidth. The ultrasound beam is set to be in x direction. Since initial ultrasound intensity and pressure delivered to the tissue is known, total acoustic reflection and attenuation can be calculated and compared between each tissue model.

2.3 Tissue Modelling

2.3.1 In-vivo tissue modelling

The mice breast tissue has been modeled to have 5 basic layers based on Sudershan et al [22]: skin, subcutaneous fat, normal mammary gland, thoracic muscle and thoracic wall to represent normal breast. For pathological model, either benign fibrosis or breast carcinoma lesion layer is added as an additional layer during calculation. Each tissue layer is having 0.5mm thickness.

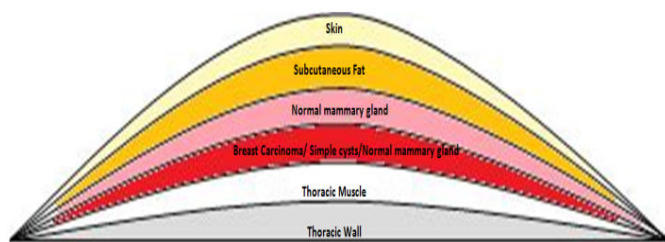


Fig. 2: Model of mice breast tissue used in the calculation

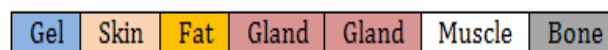


Fig 3: Normal mice breast tissue model



Fig 4: Mice breast tissue model with breast malignant lesion

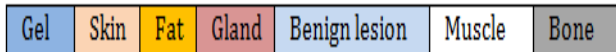


Fig 5: Mice breast tissue model with benign lesion

2.3.2 In-vitro tissue modeling

For in-vitro calculation, the mice breast model has been designed to have only the fat, mammary gland, benign fibrosis and breast carcinoma layers. The other layers are eliminated during dissection. Each tissue layer is having 0.5mm thickness.

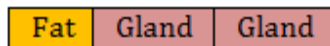


Fig 6: Normal mice breast tissue model



Fig 7: Mice breast tissue model with malignant lesion



Fig 8: Mice breast tissue model with benign lesion

Table 2 in appendix shows the acoustic and electrical parameters that were used during analysis. The properties such as ultrasound attenuation coefficient (α) and acoustic impedance (Z) is used to analyze the propagation of ultrasound wave while tissue conductivity (σ) and tissue density (ρ) is used to analyze the amplitude of magnetoacoustic voltage that rise due to the interaction between ultrasound wave and magnetic field.

2.3 Ultrasound wave propagation analysis

As ultrasound wave enters the tissue and hit tissue boundary, part of its wave will be reflected and another part of the wave will be further transmitted. The amount of reflected and transmitted ultrasound wave intensity is calculated using the following formula:

% Reflection: $(Z_2 - Z_1 / Z_2 + Z_1)^2 \times 100$, in which Z is the acoustic impedance of tissue.

% Transmission: $1 - \% \text{ Reflection}$

Inside a particular tissue layer, the transmitted ultrasound intensity is further reduced due attenuation process in that layer. Attenuation was calculated using the following formula:

$$-dB = 10 \log(I_0/I),$$

where I_0 is the initial wave intensity when ultrasound enters a particular layer and I is the intensity at the end of that layer.

These calculations were repeated every time the ultrasound wave passing through different layer of tissue to calculate the spontaneous ultrasound intensity at each layer.

2.4 Conductivity and voltage analysis

The amplitude of voltage that rises due to ultrasound wave and magnetic field interaction is calculated using equation (6) from the z axis. As instantaneous ultrasound intensity is known from the ultrasound wave propagation analysis, that instantaneous intensity is converted to instantaneous pressure at each layer following the equation: $I = p^2/Z$.

Finally, the magnetoacoustic voltage that rises in the system can be further estimated using Equation (6) with B_0 equals to 0.1T, beamwidth of 0.0254cm^2 .

3. Result

The Hybrid Magnetoacoustic method produces 2 outputs, the ultrasound echo collected by the ultrasound transducer and the magnetoacoustic voltage from the skin electrodes that rises due to the interaction between acoustic and magnetic energy. The ultrasound echo carries information with regards to tissue mechanical property such as tissue density, reflected intensity at tissue boundary and tissue acoustic attenuation whilst the magnetoacoustic voltage carries information on tissue conductivity.

3.1 Calculation Result In-vivo

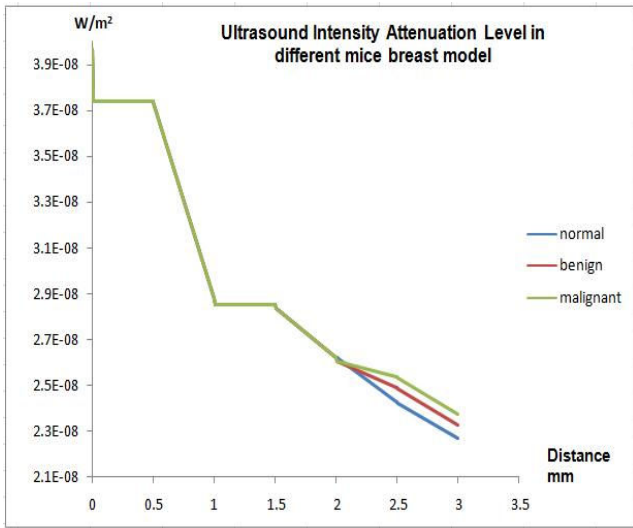


Fig 9: Ultrasound attenuation in different mice breast model in-vivo

| Breast Model | Total attenuated ultrasound intensity in-vivo (nW/m²) |
|--------------|---|
| Normal | 16.9777 |
| Benign | 16.3833 |
| Malignant | 15.930 |

Table 3: Total attenuated ultrasound intensity in-vivo

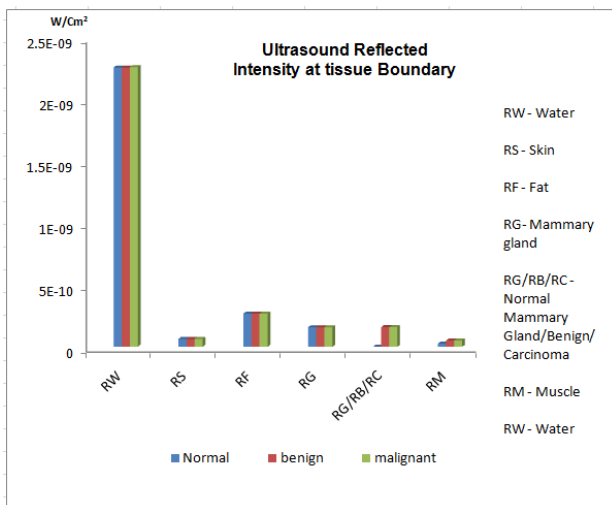


Fig 10: Ultrasound reflected at different tissue boundary in- vivo.

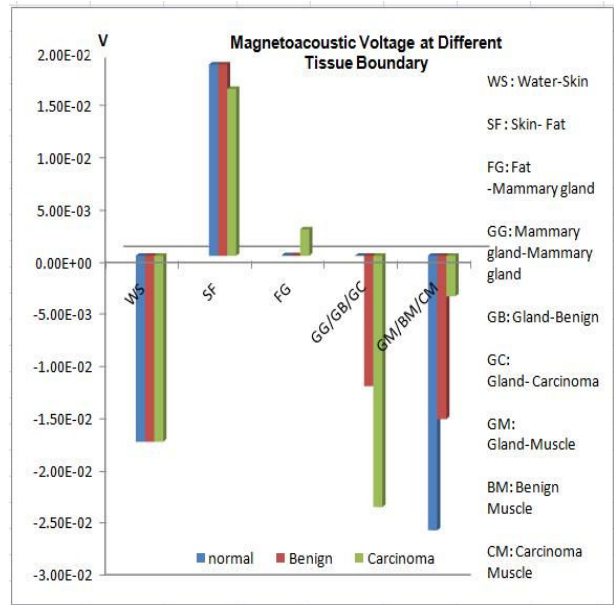


Fig 11: Magnetoacoustic voltage at different tissue boundary in vivo.

3.2 Calculation Result in vitro

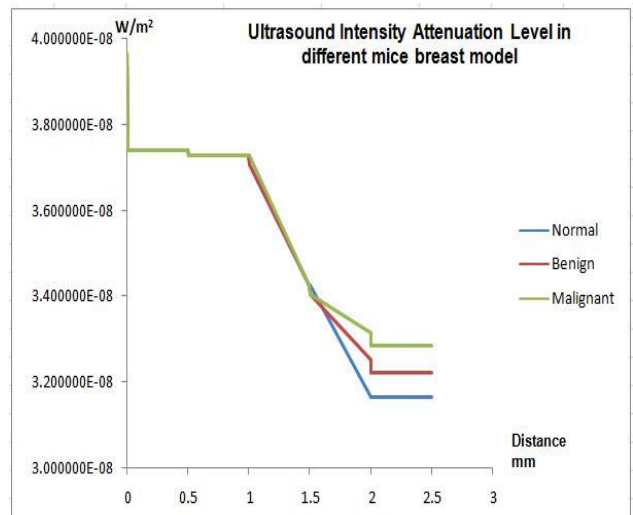


Fig 12: Ultrasound attenuation in different mice breast model in-vitro

| Breast Model | Total attenuated ultrasound intensity in-vitro (nW/m ²) |
|--------------|---|
| Normal | 7.9941 |
| Benign | 7.4245 |
| Malignant | 6.7970 |

Table 4: Total Ultrasound intensity attenuation in-vitro

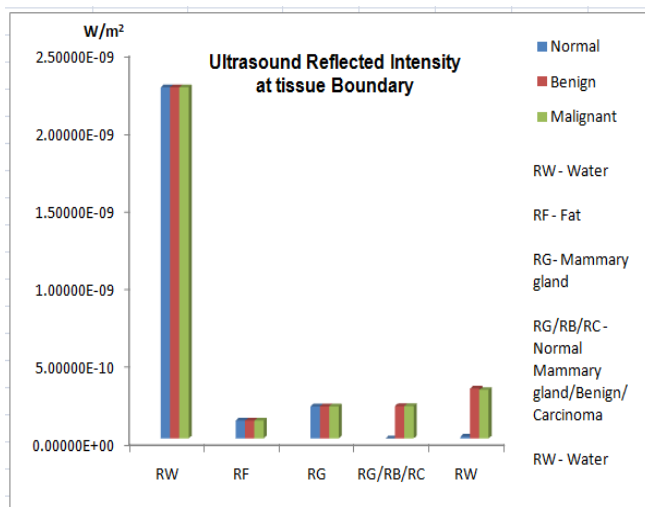


Fig 13: Ultrasound reflected at different tissue boundary in vitro

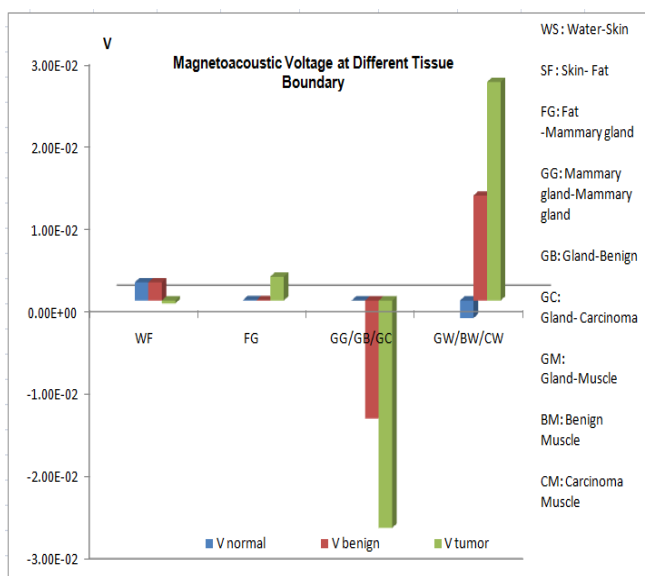


Fig 14: Magnetoacoustic voltage at different tissue boundary in-vitro.

4. Discussion

Figure 9 and 12 above respectively show the attenuation level of the mice breast models in-vivo and in-vitro. Both figures indicate that normal breast models highly attenuate ultrasound intensity within the same propagation distance followed by benign fibrosis. On the other hand, breast carcinoma models attenuate the least with about 6% reduction from normal models in-vivo and 12% reduction from normal model in-vitro. This result agrees well with the fundamental theories of ultrasound propagation in which malignant tissue with denser tissue composition will ease the propagation of ultrasound and hence, caused less attenuation. Benign fibrosis, on the other hand, is less dense than breast carcinoma and hence, attenuates some amount of sounds wave. Normal breast which is usually composed of high percentage of adipose tissue resists sound propagation and finally caused high attenuation. The total ultrasound intensity attenuated by the models is summarized in Table 3 and 4.

The ultrasound reflected intensity at tissue boundary is shown by figure 10 for in-vivo and 13 for in-vitro analysis. It includes all reflections that occur at each tissue boundaries for every mice breast models. Theoretically, percentage of reflection at tissue boundaries is determined by the level of acoustic impedance mismatch between the 2 adjacent tissues. Higher impedance mismatch will produce more reflection at the boundary and vice versa. In figure 10, in-vivo analysis shows that ultrasound is reflected at similar level for benign fibrosis and breast carcinoma since both of the tissues have the same value of acoustic impedance mismatch with their previous adjacent tissue, mammary gland. However, normal tissue model produces zero reflection since there is no tissue boundary as the adjacent layers consist of the same tissue which is also mammary gland. In-vitro reflection in figure 13 also shows the same result at the normal gland, benign and breast carcinoma layer.

The last signal collected by this system is the magnetoacoustic voltage. As shown by Figure 11 and 14, the calculation agrees well with previous research in impedance imaging, in which the amplitude of collected voltage is in the order of millivolt [1-5]. Magnetoacoustic voltage is represented by a positive and negative peak

signal at each tissue boundaries. Positive voltage amplitude indicates that the current tissue layer at that particular boundary is more conductive than the next tissue layer and vice versa as shown by signal 'GC' and 'CW' for malignant model in figure 14. Signal 'GC' is negative because the first tissue layer in that particular boundary (mammary gland) is less conductive than the next tissue layer (breast carcinoma). On the other hand, signal 'CW' is positive since the first tissue layer (breast carcinoma) is more conductive than the next layer (water).

As stated earlier, magnetoacoustic voltage produced by this system is proportional to the conductivity difference between adjacent tissues. Higher conductivity difference will produce higher voltage amplitude. From figure 14, it can be seen that, mice breast model with carcinoma producing the highest (-ve) and (+ve) voltage amplitude at both: the mammary gland-carcinoma boundary and the carcinoma-water boundary whilst normal mice breast model producing the lowest voltage amplitude at the same boundaries. Benign fibrosis, on the other hand produces moderate voltage amplitude. Despite a very clear signal amplitude differences in in-vitro analysis, in-vivo signal shows that normal mice breast model produce the highest voltage amplitude at the mammary gland-muscle layer. It also shows that the signal at malignant-muscle boundaries for malignant breast model is lower than that of normal signal because of the conductivity difference of those tissues. Hence, this amplitude indicates that conductivity difference between normal gland and muscle is much higher than the malignant and muscle. However, this complicated result can be improved by analyzing the current density within the tissue layer as an addition to voltage analysis at the tissue boundary for better tissue recognition.

The magnitude of voltage calculated in this study is an ideal value in which the direction of magnetic field, ultrasound wave and tissue interface is perpendicular to each other due to the orientation of Lorentz Force. In the real case in which tissue boundary is not fully perpendicular to the system, lower voltage amplitude may be obtained depending on the angle of the tissue interface to the system. In addition, this calculation is done on a homogenous tissue layer model. In the case of heterogenous tissue layer such as in invasive breast

carcinoma that boundaries between tissue layers is no longer distinctive, the ability of this method is not yet predicted. Modification on calculation set up and procedure such as the used of focus ultrasound transducer to focus the beam intensity within a small tissue area and improving analysis to include current density calculation will be very helpful.

4. Conclusion

Quantitative analysis on the output of Hybrid Magnetoacoustic Method for detection of normal and pathological breast tissues have been completed. 6 mice breast tissue model representing normal, breast carcinoma and benign fibrosis were used for in-vivo and in-vitro analysis. The calculation shows that, hybrid magnetoacoustic system is capable to give a distinctive output especially for in-vitro application. However, additional parameter should be considered when applying the system for in-vivo application due to the redundancy of the existing result such as to include the current density analysis. The overall output of the system is summarized in table 5.

| | Tissue | Acoustic Properties | Electric Properties |
|---------------------------------|-----------|---|-----------------------------|
| I N V I T R O | Normal | High attenuation level No ultrasound reflection | Very low voltage amplitude |
| | Malignant | Low Attenuation Level Moderate Ultrasound reflection | Very high voltage amplitude |
| | Benign | Moderate Attenuation Level Moderate Ultrasound | Moderate voltage amplitude |

| | | | |
|----------------------------|--------------------------------|---|--|
| I N V I V O | Normal | reflection | |
| | | High attenuation level | High at mammary Gland-muscle Interface (-ve) |
| | Malignant | No Ultrasound reflection | |
| | | Low Attenuation Level | Low at carcinoma -muscle layer (+ve) |
| Benign | Moderate Ultrasound Reflection | High at mammary Gland-carcinoma Interface (-ve) | |
| | Moderate Attenuation Level | Moderate voltage amplitude | |
| | | Moderate Ultrasound Reflection | |

Table 5: Summary of Hybrid magnetoacoustic system output for every breast model in-vitro and in-vivo.

References:

[1] Han Wen, Jatin Shah and Robert S. Balaban, Hall Effect Imaging, *IEEE Transactions On Biomedical Engineering*, Vol 45, No 1, 119-124, January 1998

[2] Han Wen, Eric Bennett, Jatin Shah, Robert S. Balaban, An Imaging Method using Ultrasound and Magnetic Field, *IEEE Ultrasonic Symposium*, 1997.

[3] Han Wen, Eric Bennet, The Feasibility of Hall Effect Imaging In Humans, 2000 IEEE Ultrasonic Symposium, pg 1619-1622

[4] Amalric Montalibet, Jacques Jossinet, Adrien Matias, Dominique Cathignol, Interaction Ultrasound –Magnetic field: Experimental set up and Detection of the interaction current, *2000 IEEE Ultrasonic Symposium*, pg 533-536

[5] Y. Su, S. Haider, A. Hrbek, Magnetoacousto Electrical Tomography: A new Imaging Modality for Electrical

Impedance, *2007 IFMBE Proceeding 17*, pp 292-295, 2007

[6] B. J. Roth, P. J. Bassler, J. P. Wiksowo, A Theoretical Model for Magnetoacoustic Imaging of Bioelectrical current. *IEEE. Trans.BME*. Vol 41(8), pp 723-728, 1994.

[7] Y. Su and Bin He, Magneto acoustic tomography with Magnetic Induction (MAT-MI). *Phys Med Biol*. 2005 November 7; 50(21): 5175–5187.

[8] Qingyu Ma and Bin He, Magnetoacoustic Tomography with magnetic induction: a rigorous theory. *IEEE Transaction on Biomedical Engineering*, Vol 55, No 2, Feb 2008.

[9] M. I. Mohamad Salim, M. A. Tumiran, S. N. Makhtar, B. Rosidi, I. Ariffin, A. H. Ahmad, E. Supriyanto, Quantitative analysis of Hybrid Magnetoacoustic Method for Detection of normal and pathological Breast Tissue. *Proceeding of 12th WSEAS International Conference on Automatic Control, Modelling and Simulation*, pg 144-149, 2010.

[10] Alan. J. Fann, *Breast Cancer treatment by focused microwaved thermotherapy*, Jones and Bartlette Publishers, 2007.

[11] Takahiro Sunaga, Hiro Ikehira, Shigeo Furukawa, Hiroshi Shinkai, Hirotada Kobayashi, Yoshinaga Matsumoto, Eiji Yoshitome, Takayuki Obata, Shuji Tanada, Hajime Murata and Yasuhito Sasaki, Measurement of electrical Properties of human skin and the variation among subjects with certain skin conditions. *Phys. Med. Biol*. Vol. 47, 2002, N11-N15.

[12] Thomas L. Szabo, *Diagnostic Ultrasound Imaging Inside Out*, Elsevier Academic Press, 2004.

[13] L. Landini, R. Sarnelli, Evaluation of the attenuation coefficient in normal and pathological breast tissue, *Med. and Biol. Eng. and Comput*. Vol.24, 1986,pg 243-247.

[14] Pashley, R. M, Conductivity of Pure water - De-Gassed Water is a Better Cleaning Agent (2005). *The Journal of Physical Chemistry B*, Vol.109, page 1231. [doi:10.1021/jp045975a](https://doi.org/10.1021/jp045975a)

[15] Andrzej J. Surowiec, Stanislaw S. Stuchly, J. Robin Barr and Arvind Swarup, Dielectric properties of Breast Carcinoma and Surrounding Tissue. *IEEE Transaction on Biomedical Engineering*, Vol 35, No 4, pg 257-263.

- [16] Bamber J.C, Ultrasonic Propagation properties of the Breast, *In Ultrasonic Examination of the breast*, John Wiley, Chichester, pp37-44, 1983.
- [17] The technology of Ultrasound Scanning Gel. *A Sonotech Technical Paper*, Revision 2006.
- [18] S. Gabriel, R.W. Lau and C. Gabriel, The dielectric properties of biological tissue: III. Parametric models for the dielectric spectrum of tissues. *Phys. Med. Biol.* 41(1996) 2271-2293.
- [19] P. Laugier, G. Berger and T. Baldeweck, Ultrasound Attenuation estimation in highly attenuating media: Application to skin characterization. In *Acoustical Imaging*, vol 22, Plenum Press, New York, 1996. P. Tortolli, L. Masotti (Eds)
- [20] Weiwad. Wieland, Heinig. Anke, Goetz. Linda, Hartmann. Heiko, Lampe. Dieter, Buchmann. J, Millner. R, Spielmann. Rolf Heywang-koebrunner, Sylvia. H. Direct measurements of sound velocity in various specimens of breast tissue. *Investigative Radiology*: December 2000 - Volume 35 - Issue 12 - pp 721-726
- [21] J. Jossinet, Variability of impedivity in normal and pathological breast tissue. *Med. & Biol. Eng. And Comput*, 1996,34, 346-350.
- [22] N. M. Sudarshan, E.Y. K. Ng, S. I. Teh, Surface Temperature distribution of breast with and without tumor, *Computer Methods in Biomechanics and Biomedical Engineering*, vol 2, No3, pp 187-199, 1995.
- [23] S. S Chaudary, R. K. Mishra, A. Swarup, J. M. Thomas. Dielectric properties of normal and malignant human breast tissue at radiowave and microwave frequencies. *Indian. J. Biochem. Biophys.* 21, 76-9
- [24] M. R. Stoneman, M. R. Kosempa, W. D. Gregory, C. W. Gregory, J. J. Marx, W. Mickelson, J. Tjoe and V. Raicu, Correction of electrode polarization contribution to the dielectric properties of normal and cancerous breast tissue at audio/radiofrequency. *Phys. Med. Biol.* 2007, 52, 6589
- [25] Boris Cigale, Smilijan Sinjur, Damjan Zazula, Automated Quantitative Assesment of perifollicular Vascularization Using Power Doppler Ultrasound Images. *WSEAS Transactions On Computers*, Vol 9, 2010.
- [26] Elene B. Martin, Jose M. Vega, Effect of a thin floating fluid layer in parametrically Forced waves. *WSEAS Transactions on Fluids Mechanics*, Vol 3, 2008.
- [27] Petr Dostalek, Vladimir Vasek, Jan Dolinay, Direction of sound waves arrival determination using time-delay and beamforming method, *WSEAS Transactions on circuit and system*, Vol 8, 2009.

Appendix

| Tissue | α reference value (dB/cm/MHz) | α calculated value (dB/0.5mm/10MHz) | Acoustic Impedance (Z) Mrayls | Conductivity (σ), S/m @ (1-27MHz) | Density (ρ) kg/m ³ |
|--|--|--|-------------------------------|--|--------------------------------------|
| Transducer Matching layer | - | - | 2.41 | | |
| Water | 2.17e-3 @2 MHz [12] | 5.425 e-4 | 1.482 [12] | 0.0001 [18] | 1.000 [12] |
| Skin | 2.25 @ 1MHz (average dermis and hypodermis) [19] | 1.125 | 1.61[17] | 0.5 [18] @10MHz | 1000 [9] |
| Fat | 0.738 @ 10MHz [13] | 0.0369 | 1.327 [12] | 0.1 [15] @ 10MHz | 928 [12] |
| Gland/parenchyma of cancerous breast/far from tumor center | 6.845@ 10MHz [12] | 0.3422 | 1.540 [12] | 0.07 [15] | 1020 [10] |
| Normal breast tissue/Fibrofatty parenchyma | 6.845@ 10MHz [12] | 0.3422 | 1.540 [12] | 0.05 [15] | |
| Benign Fibrosis | 3.98@ 10MHz [13] | 0.199 | 1.8 [10 x 16], [20] | 0.393[21] | 1030 [10] |
| Breast Carcinoma | 2.33@ 10 MHz[13] | 0.1165 | 1.8 [10 x 16][20] | 0.8[24][23][15] @ 10MHz | 1041[10] |
| Muscle | 0.57 @ 1MHz [12] | 0.285 | 1.645 [12] | 0.8 [11] @ 10MHz | 1041[10] |
| Bone | 3.54@ 1 MHz [12] | 1.77 | 6.364 [12] | 0.05 [11] @ 10MHz | 1990 [12] |

Table 2: Overall acoustical and electrical tissue properties used in the calculation